Development and evaluation of a novel designed breast CT system

Claudia Braun^a, Helmut Schlattl^a, Oleg Tischenko^a, Olaf Dietrich^b and Christoph Hoeschen^a

^aHelmholtz Zentrum München, Research Unit Medical Radiation Physics and Diagnostics,

Ingolstädter Landstr. 1, 85764 Neuherberg, Germany

^bLudwig-Maximilians-University Hospital Munich, Institute for Clinical Radiology, Marchioninstr.

15, 81377 Munich, Germany

ABSTRACT

The performance of a novel designed x-ray CT scanning geometry is investigated. Composed of a specially designed tungsten collimation mask and a high resolution flat panel detector, this scanning geometry provides high efficient data acquisition allowing dose reduction potentially up to 50%.

In recent years a special type of scanning geometry has been proposed. A first prototype of this geometry called CT-DOR(CT with Dual Optimal Reading) has already been built. Despite many drawbacks, resulting images have shown promising potential of dual reading. The approach of gaining two subsets of data has anew been picked up and come to terms with a novel designed CT scanner for breast imaging. The main idea consists of collimating the X-ray beam through a specially designed shielding mask thereby reducing radiation dose without compromising image quality. This is achieved by hexagonally sampled Radon transform and image reconstruction with the especially suitable OPED (orthogonal polynomial expansion on disk) algorithm. This work now presents the development and evaluation of the novel designed breast CT system. Therefore simulated phantom data were obtained to test the performance of the scanning device and compared to a standard 3rd generation scanner. Retaining advantages such as scatter-correction potential and 3D-capability, the proposed CT system yields high resolution images for breast diagnostics in low energy ranges. Assuming similar sample size, it is expected that the novel designed breast CT system in conjunction with OPED outperforms the standard 3rd generation CT system combined with FBP (filtered back projection).

Keywords: CTDOR, parallel interlaced, OPED

1. INTRODUCTION

The early and accurate diagnosis of breast cancer in women is still an important topic of current research. Today's state of the art in breast imaging is digital x-ray mammography. However, this method suffers from several insufficiencies. Most importantly, sensitivity in lesion detectability is variable and inversly proportional to breast density. In patients with dense breast, sensitivity can be as low as 30 to 48% with much higher interval cancer rates.¹

Several imaging modalities are under investigation to improve diagnostic performance. One of these approaches is dedicated breast computed tomography (CT). Aiming at 3D imaging, it should overcome superpositioning of structures. Beside that, breast CT has to face several demands like low patient doses in ranges of two-view mammography-scans and good soft-tissue differentiation. On the other hand high resolution of $100\mu m$ is also necessary to detect microcalcifications.

The idea of the proposed breast CT system has evolved from a special type of scanner geometry presented at SPIE Medical Imaging 2006.² It rests upon a full circle collimation mask with equally spaced windows and shielding elements. Inherently, this type of geometry enables up to 50% dose reduction without compromising image quality.² A first implementation has been done in the form of a prototype called CTDOR (CT with dual optimal reading).³ As the name says, two groups of detectors have been used in order to yield two complementary subsets of data. Despite many drawbacks, such as different detector response, low image resolution and 2D-capability only, resulting images have shown promising potential of dual reading. In present work, The idea of dual reading has anew been picked up and came to terms with a novel designed CT scanner for breast imaging.⁴

Correspondence to C.B. (claudia.braun@helmholtz-muenchen.de)

2. MATERIALS AND METHODS

2.1 Principles of CTDOR

In CT data are acquired in form of integrals measured along lines traversing the object. A spatial configuration of all lines of integration is referred to as either the geometry of the data or the scanning geometry. Reconstructions itself can be further subdivided in geometry-unconditioned algorithms like algebraic reconstruction technique) and algorithms that depend strongly on the scanning geometry. Among these approaches are the most widely used the filtered backprojection algorithm (FBP) and a recent developed reconstruction algorithm called OPED (orthogonal polynomial expansion on disk).

It is further interesting to note that sampling the projections at all points is not necessary. Rattey and Lindgren⁶ found that an interlaced parallel geometry, defined by a hexagonal grid (see Fig.1), has the same resolution as the rectangular grid, which is sampled at each data point. More specifically, one has to sample the projections only at those points p_j for which p+j is even i.e. at odd j for odd-numbered projections and at even j for even numbered projections. Such an interlaced parallel geometry is not only very efficient, it is the optimum among all fan beam geometries.⁷

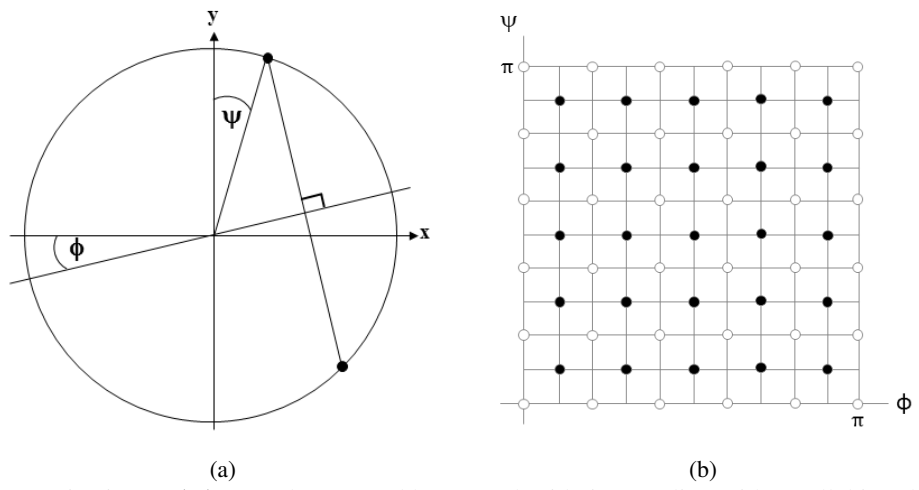


Figure 1: Parameterization to ϕ, ψ (a) and generated hexagonal grid via sampling with parallel interlaced geometry

CTDOR utilizes precisely this given fact to achieve the same image quality while reducing dose to 50%. Introducing the coordinates ϕ for the projection angle and the parameter ψ defining the position of the ray within one projection, a hexagonal grid can be generated if sampling is done over stripes that connect either two windows, denoted the second kind of data or connecting window and shielding element. These stripes are assigned to the first kind of data and are marked as black dots in Fig.1. The second kind of data, in turn, is indicated with white circles. Both kinds can be reconstructed separately with OPED. In doing so, N rays in one projection of the first kind data set are distributed according to zeros of Chebyshev polynomials of first of order N, whereas second kind data distribution coincides with zeros of Chebyshev polynomials of second kind and of order N-1.8

2.2 Scanning device

Similar to the 3rd generation CT scanners, source and detector of the proposed CT geometry are co-rotating around the object, whereupon the mask collimators remain stationary. Traversing radiation is collected by the flat-panel detector that is placed inside a shielding ring mask. Its pixel size is about one order of magnitude lower than the size of absorbing elements and windows respectively. Assuming that windows and shielding elements are represented as points uniformly distributed over a circle, whereas the number of windows is denominated as N, the two sub-sets of data are collected by the configuration of the stripes connecting 2N points. The assignment of collected data to the interlaced parallel geometry is done by sinusoidal lateral sampling. In doing so the integral value measured by a flat panel detector makes contribution to the chord connecting the points ψ_1 and ψ_2 (see Fig.2).

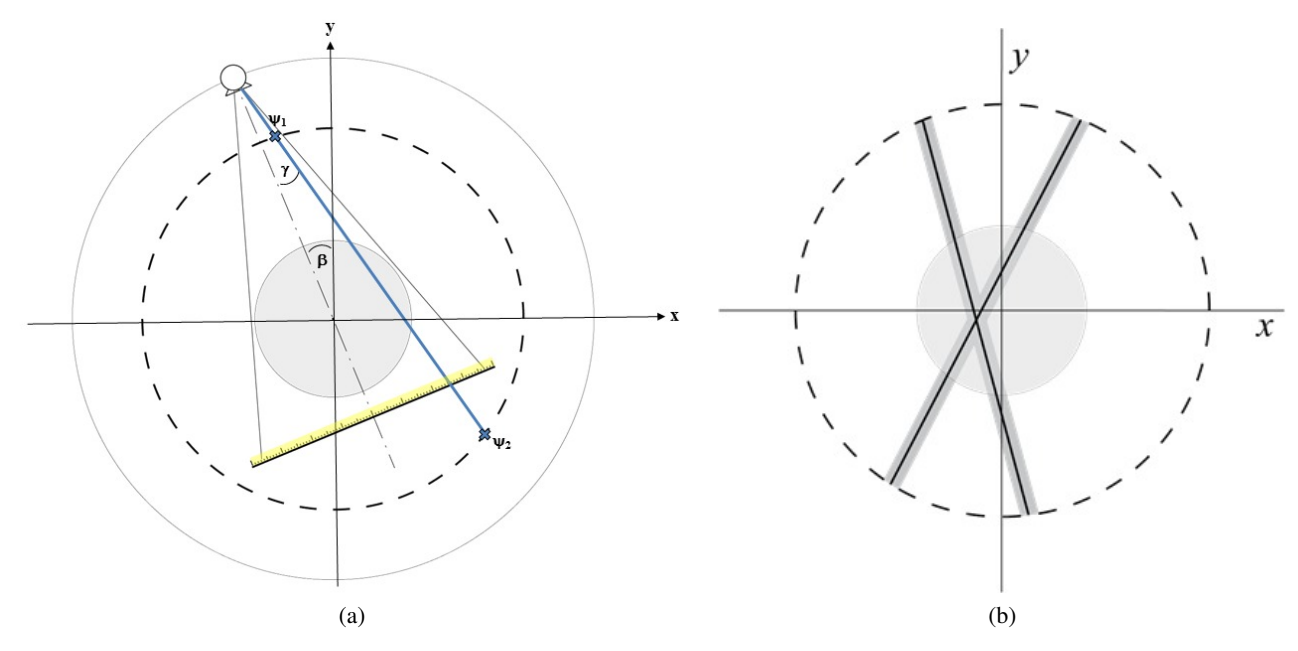


Figure 2: Data acquisition method with the use of a flat panel detector placed inside a shielding mask(a) and one example each of resulting first kind and second kind chords(b)

2.3 Simulation studies

In order to test the scanner performance setup parameters similar to the CAD design (compare 3.1) were taken and implemented into Geant4.9.6 source code geometry. Experimental data is generated with the help of a phantom model described below and Monte-Carlo simulation. The energy spectrum chosen for this study corresponds to a tube voltage of 50kV with a filtration of 0.5mm Al and 0.11mm Cu (see Fig.3. For simulation of our demonstrator and for standard flat panel breast CT the histories of 10^{10} photons have been followed up, considering photo effect, Rayleigh and Compton scattering. The path of one photon has been tracked until their energy falls below 5keV. The CsI detector is considered to be linearly responding. Both Monte-Carlo studies, for CTDOR scanning geometry and for the standard 3rd generation scanner, were conducted with the same parameter settings, as listed in table 1.

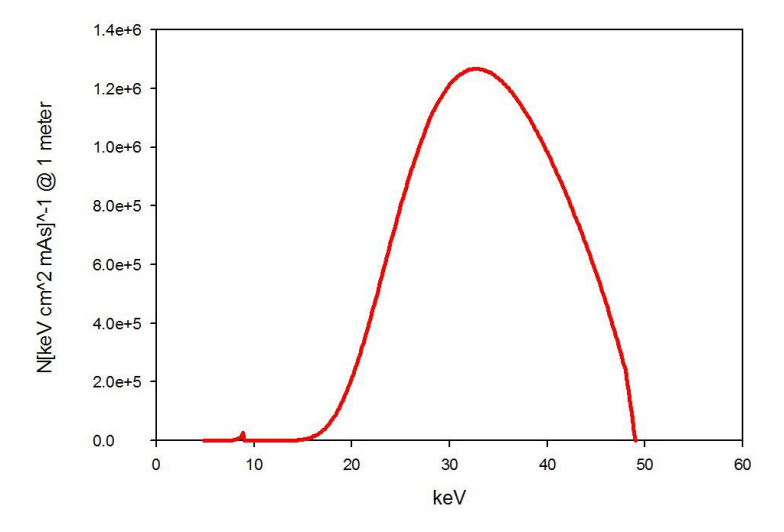


Figure 3: X-ray spectrum used for Monte-Carlo simulations

	CTDOR	3rd Generation
Number of histories	$1.08 \cdot 10^{10}$	$1.08 \cdot 10^{10}$
Resolution element	0.3mm	0.3mm
Focal spot size	0.07mm	0.07mm
Source Detector Distance	294mm	294mm
Source Isocenter Distance	181mm	181m
Number of Views	3600	3600

Table 1: Parameters for Monte-Carlo simulations

Since 1800 tungsten shielding elements (see also 3.1 for details) in Monte-Carlo evaluation are very CPU time consuming, the simulated data for CTDOR is generated similar to standard geometry with afterwards setting one half of simulated data to zero. More precisely, those data points that correspond to a hit with shielding elements previous to the object (see also fig.2) are considered to be of zero value. In this way one achieves at about one half of dose for the case of CTDOR compared to 100% of dose for standard scanner geometry. Thus, it is possible to oppose the novel designed low dose breast CT system to standard approaches.

The cylindrical phantom used for this simulation studies is depicted as traverse slice in fig.4. It is filled with adipose tissue and is of diameter size 60mm. Microcalcifications were put into adipose tissue in diameter sizes of $500\mu m$ (see fig.4 Mi.1-Mi.6). They are considered to be composed of hydroxyl apatite with a density of $3.14g/cm^3$. To see further how soft tissue inserts (compare fig.4: S.1 3mm, S.2 2mm, S.3 1mm, S.4 0.5mm) and breast tissue components (compare fig.4: B.1 10mm, B.2 6mm, B.3 4mm) are visualized, they are also placed into adipose tissue with different diameter sizes. In order to visualize microcalcifications, linear branched and pleomorphic on the one hand and the differentiation of embedded tissue on the other hand, some of them were placed into breast tissue components (compare fig.4: BMi.1 and BMi.2) in different sizes and also branching.

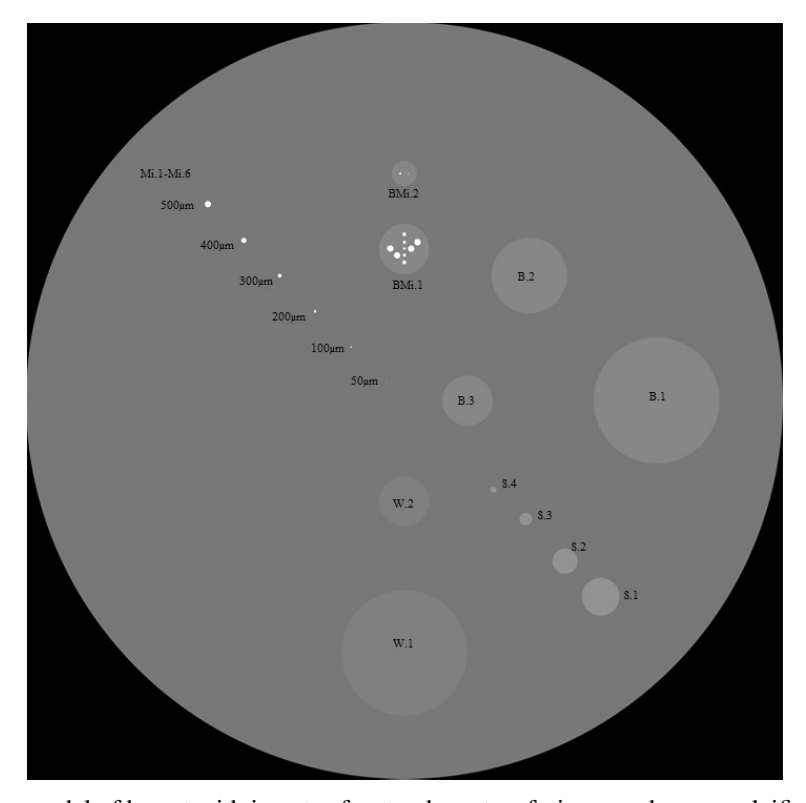


Figure 4: Traverse slice model of breast with inserts of water, breast, soft tissue and macrocalcifications in adipose tissue

3. RESULTS AND DISCUSSION

3.1 Computer-aided design of the demonstrator

The proposed cone-beam breast CT demonstrator is realized as a modular, bench-top CT-system, meaning x-ray source and detector remain stationary whereas object and the shielding mask are rotating. Rotation itself is done by a precision rotation stage PRS200 (Pimicos, Germany). It can be seen in Fig.5 positioned under the purpose-built light-weight constructed rotation table guiding the object and the shielding mask. This special construction is needed to avoid errors in precision staging and further to enable the adjustment of the system by using a micrometer cross stage. This stage is placed between the rotation table and rotation stage.

The x-ray source is a computer controlled tungsten x-ray tube (OXFORD INSTRUMENTS, UK) with 0.07mm focal spot size. It can be operated at up to 50kVp with 1mA maximum tube current. Different copper and aluminium filters can be placed in a holder in front of the tube window.

For x-ray detection a high resolution CMOS-based detector (DEXELA, UK) is used, providing a matrix of 1536x864 pixels each of $0.075mm^2$ size. A structured scintillator plate of 0.15mm thickness is placed on a Fibre optic plate that guides light while blocking incident x-rays. The signal digitization is 14bits/pixel while DQE is of 0.7 at 0.5lp/mm. The flat-panel detector can be operated with 60 frames per second at full resolution.

The shielding mask is made of high absorbing material tungsten with 1800 window and 1800 shielding elements, each being of size 0.3mm. The hexagonal shape as pictured in Fig.6 has been selected to achieve the best penumbra.⁴

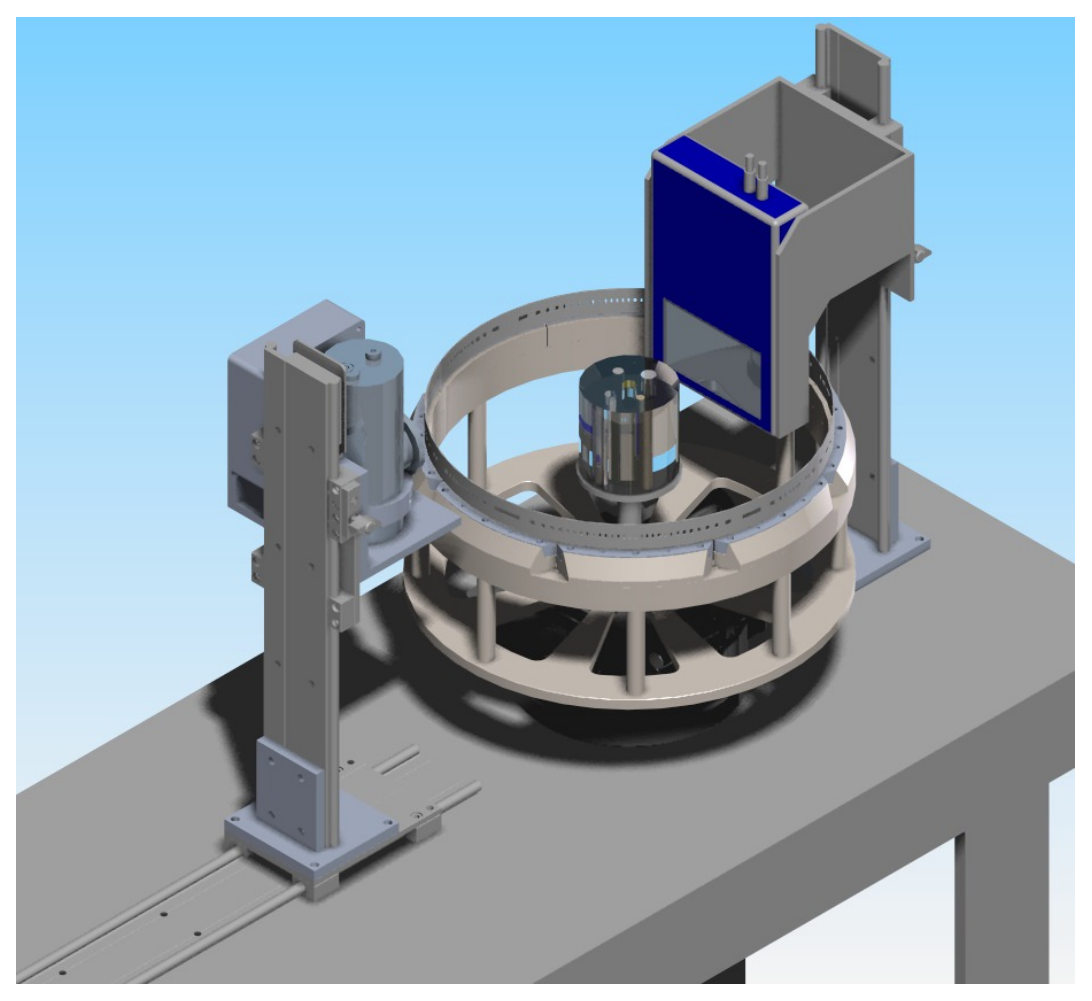


Figure 5: Computer-aided design of the proposed CTDOR-based breast CT demonstrator

Proc. of SPIE Vol. 9033 903311-5

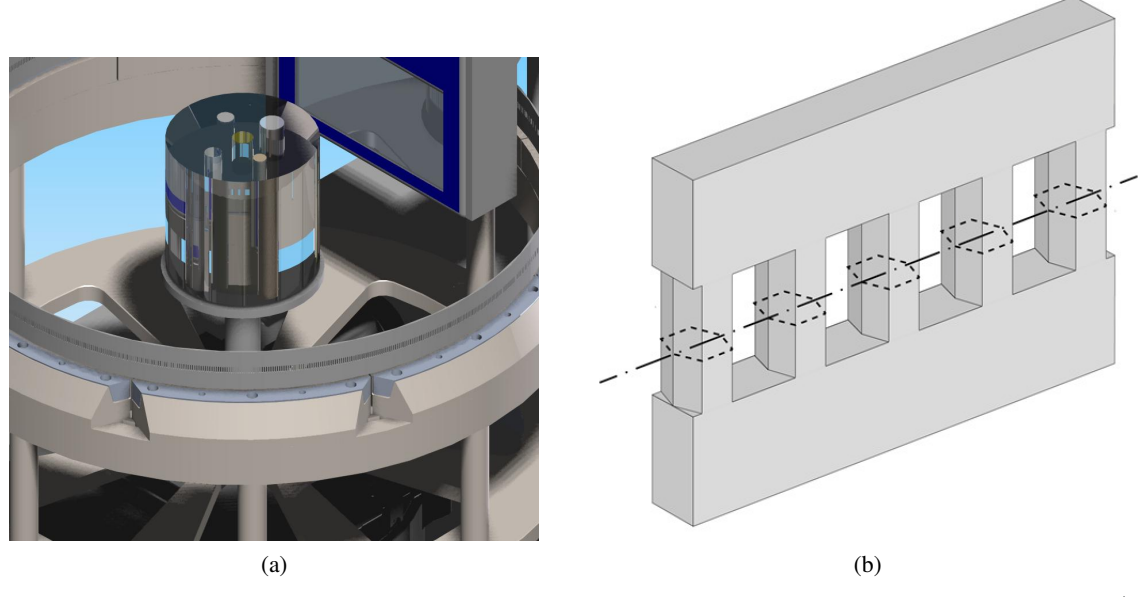


Figure 6: Magnified view on the shielding mask (a) and how it is structured to obtain the best penumbra⁴ (b)

3.2 Reconstruction of Datasets

Simulated phantom data are sampled in a way to obtain first and second kind Radon data. Both were reconstructed separately with OPED. Fig.7(a,b) shows the reconstruction of first and second kind data. In both cases microcalcifications of sizes down to 0.2mm are clearly visible, although not fully resolved. For both kinds, the existence of artifacts caused by insufficient sampling can be seen. These artifacts, however, diminish if both reconstruction are added (see Fig.7(c)). Besides that, it is also possible to join the two complementary datasets to a complete radon data set and reconstruct the whole set of achieved data. Compared to the addition of separate reconstructions the reconstruction of the whole data further results in a better resolution. Low contrast details are all visible to a size of 0.5mm (note inserts S.4) in all versions of reconstruction. Some ring artifacts are also on display. The reason for this lies in the assignment of the flat detector on the individual strips. This, however, can be either improved or eliminated by geometric optimization of the assignment process. This may also be the reason for the partial volume artifacts that occur near the edge of microcalcifications. They can also be interpreted as beam hardening artefacts, but, considering that, the reconstruction with FBP (see fig.8) should suffer from the same. This is however not the case.

3.3 Comparison to Standard CT

Both geometries, CTDOR in combination with OPED and the 3rd generation CT scanner in combination with FBP, result in images of high resolution, where the CTDOR achieves slightly higher resolution than standard 3rd generation scanner with FBP. The artifacts from which the reconstruction of CTDOR with OPED currently suffers from, i.e. rings and streaks near the edges of microcalcifications, arise from the the assignment process to stripes and can be eliminated or even improved by optimizing this process. Both reconstructions variants can visualize soft tissue inserts (note insert S.4) of size 0.5mm. Considering the fact that CTDOR delivers the same or even better resolved images with applying only one half of dose, CTDOR outperforms standard 3rd generation scanner geometry.

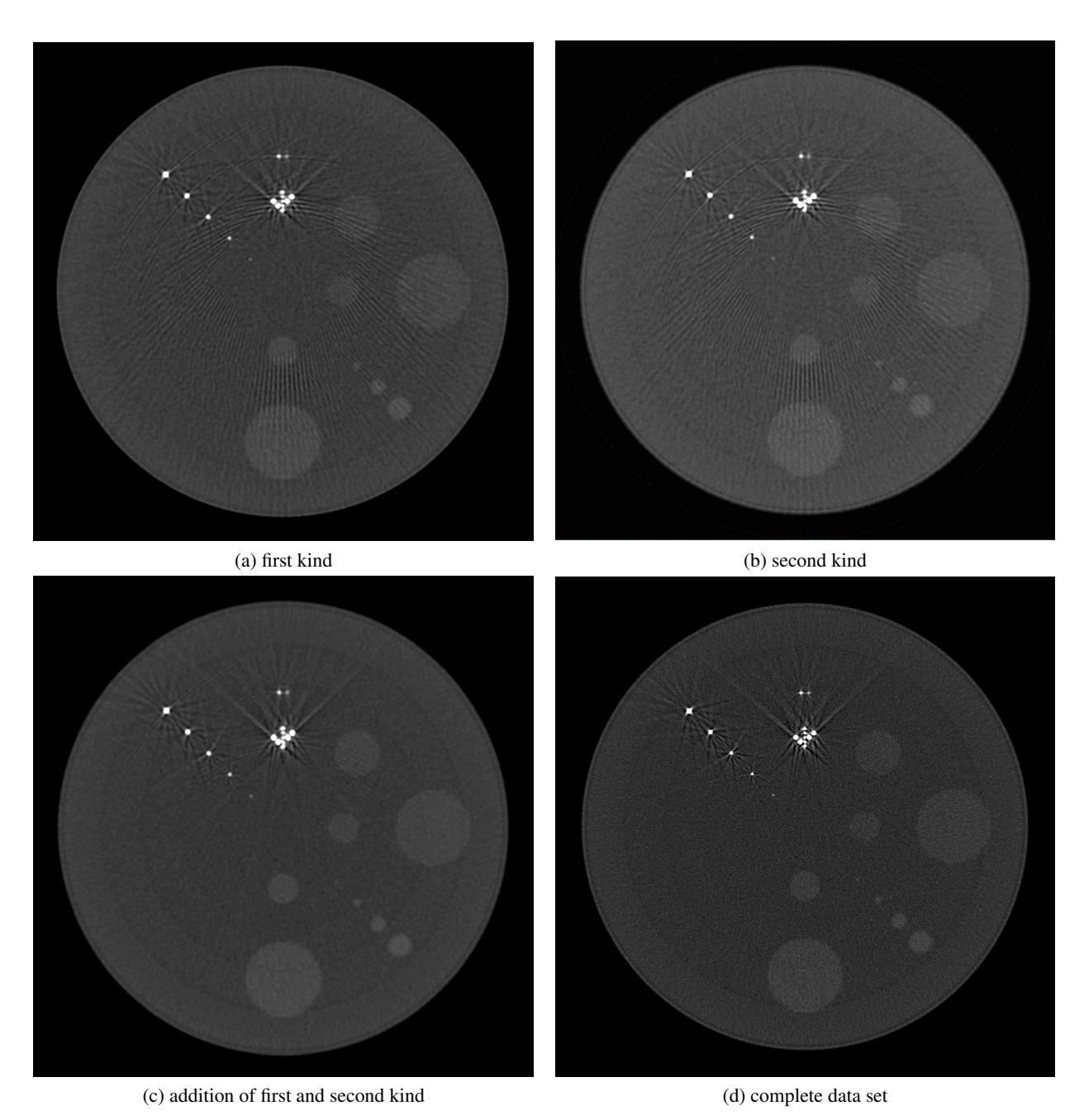
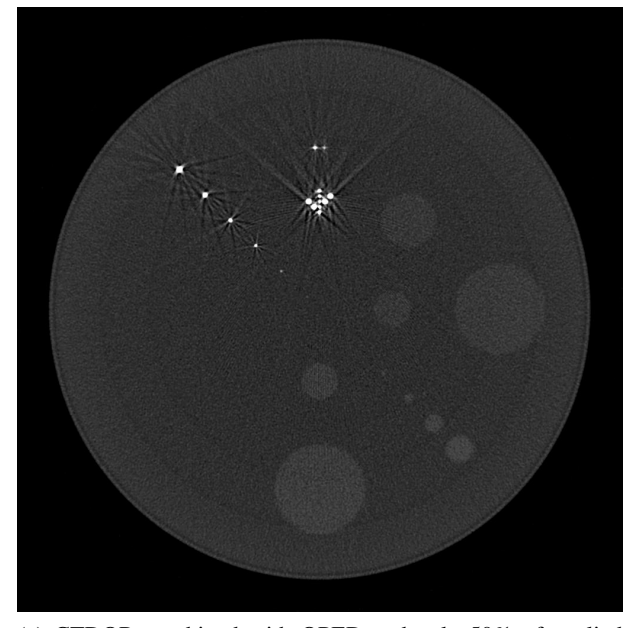
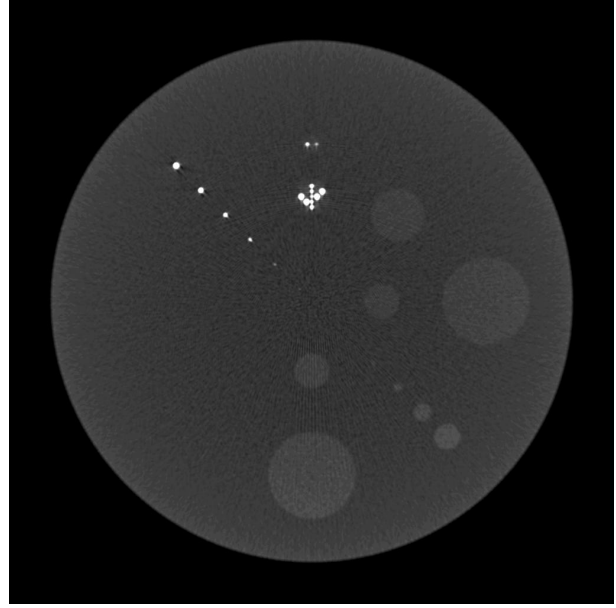


Figure 7: Reconstruction with OPED





(a) CTDOR combined with OPED and only 50% of applied dose

(b) 3rd generation combined with FBP

Figure 8: Comparison of CTDOR with standard CT geometry

4. CONCLUSIONS

The present work shows that, in energy ranges of 50kVp, it is possible to resolve microcalcification of at least 0.3mm and to visualize soft tissue inserts of 0.5mm. Considering the fact that CTDOR in combination with OPED achieves same or better resolved images, the novel development geometry outperforms the standard 3rd generation CT geometry combined with FBP. Remaining artifacts due to assignment of collected data to stripes can be improved or eliminated by optimizing this process. Aliasing artefacts can further be diminished by the superposition of the separately reconstructed images of first and second kind data.

The development of a new geometry in conjunction with the newly developed reconstruction algorithm OPED therefore is pursued further and will be implemented into reality with the help of the developed CAD designs.

A detailed analysis of image quality metrics concerning spatial resolution and noise are the next steps in near future. It is also important to note, that the necessary evidence of results being the same, including scattering processes and incomplete absorption arising at the edges of shielding elements, has to be provided by experimental results.

ACKNOWLEDGMENTS

The work of the first author was supported by HELENA - Helmholtz Graduate School of Environmental Health.

REFERENCES

- 1. Carcaci, S. and Santiago, L., [Role of Mammography in Screening for Breast Cancer: Is it still the Gold Standard?], SPIE Press (2012).
- 2. Tischenko, O., Xu, Y. and Hoeschen, C., "A new scanning device in ct with dose reduction potential," Proc. SPIE 6142 61422L (2006).
- 3. de las Heras, H., Tischenko, O., Schlattl, H., Xu, Y. and Hoeschen, C., "Modelling and testing of a non-standard scanning device," Proc. SPIE 6510 6510R (2007).
- 4. Braun, C., Tischenko, O., Giedl-Wagner, R., Schlattl, H. and Hoeschen, C., "Mask collimation meets high -efficient data acquisition: A novel design of a low-dose-ct-scanner for breast-imaging," Proc. SPIE 8668 8668H (2013).
- 5. Tischenko, O. and Hoeschen, C., [Reconstruction Algorithms and Scanning Geometries in Tomographic Imaging], Springer-Verlag Berlin Heidelberg (2013).

- 6. Rattey, P. and Lindgren, A., "Sampling the 2-d radon transform," IEEE Trans. Acoust. Speech Signal Processing 994–1002 (1981).
- 7. Natterer, F., "Siam j. appl. math," Sampling in fan beam tomography (2), 358–380 (1993).
- 8. Tischenko, O., Xu, Y., Goetzfried, T., Bogner, L. and Hoeschen, C., "Reduction of aliasing artifacts in ct images," Proc. SPIE 7258 72583F (2009).

Proc. of SPIE Vol. 9033 903311-9